Ground Water Monitoring&Remediation

Moderate Bioclogging Leading to Preferential Flow Paths in Biobarriers

by Katsutoshi Seki, Martin Thullner, Junya Hanada, and Tsuyoshi Miyazaki

Abstract

Permeable reactive barriers (PRBs) are an alternative technique for the biological in situ remediation of ground water contaminants. Nutrient supply via injection well galleries is supposed to support a high microbial activity in these barriers but can ultimately lead to changes in the hydraulic conductivity of the biobarrier due to the accumulation of biomass in the aquifer. This effect, called bioclogging, would limit the remediation efficiency of the biobarrier. To evaluate the effects bioclogging can have on the flow field of a PRB, flow cell experiments were carried out in the laboratory using glass beads as a porous medium. Two types of flow cells were used: a 20- × 1- × 1-cm cell simulating a single injection well in a one-dimensional flow field and a 20- × 10- × 1-cm cell simulating an injection well gallery in a two-dimensional flow field. A mineral medium was injected to promote microbial growth. Results of 9 d of continuous operation showed that conditions, which led to a moderate (50%) reduction of the hydraulic conductivity of the one-dimensional cell, led to a preferential flow pattern within the simulated barrier in the two-dimensional flow field (visualized by a tracer dye). The bioclogging leading to this preferential flow pattern did not change the hydraulic conductivity of the biobarrier as a whole but resulted in a reduced residence time of water within barrier. The biomass distribution measured after 9 d was consistent with the observed clogging effects showing step spatial gradients between clogged and unclogged regions.

Introduction

The efficiency optimization of in situ ground water remediation as well as the minimization of costs and risks of such remediation measures is an active field of research for science and engineering. Among other techniques, e.g., pump-and-treat or monitored natural attenuation, permeable reactive barriers (PRB) have been proposed for the in situ remediation of contaminated ground water. The basic principle of this technique is to install a reactive zone downgradient of the source of contamination. Until now, the majority of PRBs are based on the abiotic degradation of contaminants using variable reactive media depending on the target contaminants (Scherer et al. 2000). However, during the past years there has been a considerable increase in studies focusing on engineered PRBs making use of the microbial remediation of contaminants (Kalin 2004). Techniques to construct a PRB depend on the reactive material used as well as on the site conditions. Microbial PRBs were either installed by excavating parts of the aquifer and refilling the reactive material (Gavaskar 1998), or by installing well arrays, which supply substrates supporting microbial growth and activity (e.g., Dybas et al. 2002). The main advantage of PRBs compared to other remediation techniques is that after installation of the barrier only limited activities are required, e.g., periodical injection of reactive material and monitoring of performance. Thus, the longevity of a PRB is an important issue for the efficiency of this remediation technique. There are two main factors leading to a reduced PRB efficiency: first, the reactivity of the reactive material can become exhausted, and second, the permeability of the barrier can not be maintained, i.e., contaminants can bypass the reactive zone without being degraded.

Processes potentially reducing the long-term permeability of a PRB include the physical (e.g., particle deposition), chemical (e.g., mineral precipitation), and biological (e.g., biomass buildup or microbial gas production) clogging of the reactive zone. The latter process is of increased relevance for microbial PRBs as the buildup of a sufficient amount of biomass is a necessary prerequisite for the bioremediation of the contaminants. Microbially induced clogging has been observed in many natural or artificial porous media (Baveye et al. 1998), e.g., at the bottom of waste water infiltration ponds (Davis et al. 1973), at septic tank effluents (Kristiansen 1981), or in the vicinity of ground water discharge wells (van Beek and van der Kooij 1982). More relevant for PRBs, the injection of substrates, which promote microbial growth in an aquifer, is known to

clog waste water injection wells (e.g., Oberdorfer and Peterson 1985) or artificial recharge wells (e.g., Rebhun and Schwarz 1968; Vecchioli 1970). Furthermore, injecting growth-promoting substrates into an aquifer in order to enhance the bioremediation of contaminants can also lead to microbially induced clogging of the vicinity of the well, which reduces the efficiency of this well significantly (McCarty et al. 1998). In contrast, injecting growth-promoting substrates into an aquifer via well galleries is a technique to establish impermeable subsurface barriers making use of the microbial clogging—or bioclogging effect (Trefry et al. 1998; Hiebert et al. 2001). Therefore, bioclogging might also occur around well galleries used to install microbial PRBs, severely challenging their remediation performance. Unfortunately, only little is known on bioclogging of PRBs under field conditions because controlled experiments that address the significance and extent of such phenomena on the hydrodynamic characteristics of PRBs are lacking (Scherer et al. 2000).

In contrast, bioclogging has been investigated in several laboratory studies showing that in columns or flow cells with a one-dimensional flow field the growth of biomass can lead to severe reductions of hydraulic conductivity of the system (e.g., Taylor and Jaffé 1990; Cunningham et al. 1991; Vandevivere and Baveye 1992a; Seki et al 1998). Furthermore, it has been shown in flow cells having a two-dimensional flow field that bioclogging in the vicinity of an injection well can lead to significant changes in the flow field causing a flow bypass of the clogged zone without changing the average hydraulic conductivity of the entire system (Kildsgaard and Engesgaard 2002; Thullner et al. 2002a). Extrapolating the latter observations to the field scale implies that bioclogging might limit the performance of a PRB without necessarily being recognized by the monitoring system of the PRB.

Up to now, an explicit comparison with conditions leading to the bioclogging of a column and conditions leading to the flow bypass of a bioclogged zone has not been done. Addressing this question would help verify the ability of predicting the risk for bioclogging occurring in a PRB based on the results of laboratory studies. Furthermore, the investigation of a clogged laboratory-scale biobarrier would help to determine criteria, which can be used to determine the occurrence of bioclogging in the field.

The objective of this study is to investigate the conditions leading to a bioclogging-induced flow bypass of an injection well. Results on the bioclogging in flow cells with one-dimensional and with two-dimensional flow fields were compared to clarify to what extent the processes in a two-dimensional flow field, typical for a biobarrier, might be predicted based on column experiments.

Materials and Methods

Setup and Operation of the Flow Cells

Experiments were conducted in two different flow cells. Flow cell A (Figure 1 top: length 20 cm; width 1 cm; thickness 1 cm) simulating a one-dimensional flow field and cell B (Figure 1 bottom: length 20 cm; width 10 cm; thickness 1 cm) simulating a two-dimensional flow field. Both flow cells were made of light transparent acrylic plastic material and were uniformly packed with glass beads of 0.1-mm mean diameter resulting in a bulk density of 1.59 Mg/m^3, which corresponds to total porosity of 0.383. Inlet and outlet of the flow cells were supported by 0.1-mm nylon mesh screens. The inflow and the outflow of the flow cells (one port each for flow cell A and three ports each for flow cell B) were kept at a constant pressure head with a head difference between inlet and outlet of 6 cm resulting in an average hydraulic gradient along the flow cells of 0.3. Additional injection ports were installed in flow cell A at 4 cm distance (tracer injection port) and in flow cells A and B at 10 cm distance from the inlet (nutrient injection ports). At the bottom of both flow cells, water manometers were installed for monitoring the local distribution of the pressure heads. The manometers were located at 4, 7, 10, 13, and 16 cm from the inlet. Flow cell A was equipped with one row of manometers and one nutrient injection port, whereas flow cell B was equipped with three parallel rows of manometers (with 3-cm distance between each manometer row and 2-cm distance between the outer manometers and the wall of the flow cell; Figure 1 bottom) and three tracer and nutrient injection ports each.

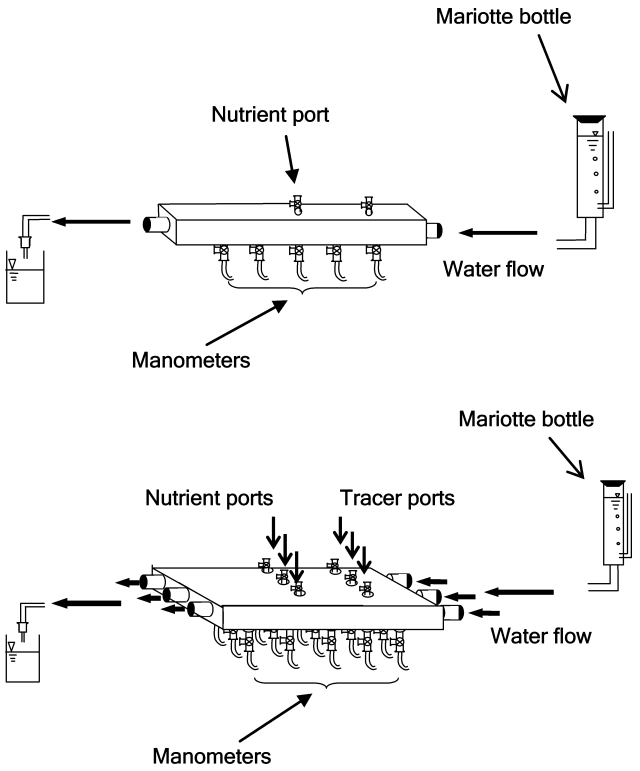

Figure 1. Setup of flow cell A (top) and flow cell B (bottom).

Each flow cell was operated under water-saturated conditions, in horizontal position, and at a constant temperature of 20°C. After packing, the inoculum was injected into the nutrient injection ports. This injection lasted until a 2-cm region around the injection ports was inoculated using Brilliant Blue FCF dye in the inoculum to determine the inoculated area visually. After 24-h incubation time, continuous flow was started. Deionized water was supplied

to the inlet ports, and the mineral medium was supplied to the nutrient injection ports using Mariotte bottles, both kept at the same pressure head. Brilliant Blue FCF dye was dissolved in the nutrient solution to observe the flowpath of the mineral medium. Discharge rates were measured to calculate average fluxes in the flow cells, and for flow cell A hydraulic conductivity was calculated from the measured flux and manometer readings. When measuring discharge rates, the injection of the mineral medium from the nutrient injection ports was stopped and deionized water was supplied to the inlet ports only.

Every other day the mineral medium in the Mariotte bottle was replaced with a fresh autoclaved medium solution, and tubings between the Mariotte bottle and the injection ports were flushed for cleaning.

Tracer tests were performed in flow cell B after 1.9, 2.9, 6.8, and 8.8 d of continuous flow operation. During each tracer test, the mineral medium flow and the background flow through the inlet ports were stopped and a pulse of tracer solution using Brilliant Blue FCF dye was injected into the three tracer injection ports. After injecting the tracer pulse, the background flow started again being the only flux source throughout the tracer test. Tracer distribution was monitored by taking photos from the top of the flow cell using a digital camera.

The experiments were finished after 9 d of continuous flow operation.

Growth Medium and Inoculum

The mineral medium consisted of glucose, 1.0 g/L; egg albumin, 0.25 g/L; K_2HPO_4, 0.5 g/L; $MgSO_4$ $7H_20$, 0.2 g/L; and trace amount of $Fe_2(SO_4)_3$ dissolved in deionized water. The pH of the medium was adjusted to 6.8 to 7.0. The medium was autoclaved before supplying injection into the flow cells.

The inoculum was made from a mixture of soil (Andisol) and the mineral medium to simulate microbial fauna in natural soil environment, resulting in 10 g of the soil medium mixture containing 1 g of dry soil. The numbers of the bacteria in the soil were 2.94×10^6 cells/(g soil); thus, the inoculated medium contained 2.94×10^5 cells/cm^3.

Microbial Count

After the flow was terminated, numbers of bacteria and fungi were measured by the dilution spread plate count method (Weaver et al. 1994). The growth medium used for bacteria counting consisted of glucose, 1.0 g/L; egg albumin, 0.25 g/L; K_2HPO_4, 0.5 g/L; $MgSO_4$ $7H_20$, 0.2 g/L; trace amount of $Fe_2(SO_4)_3$; and agar, 15 g/L dissolved in deionized water. The pH of the medium was adjusted to 6.8 to 7.0. The growth medium used for fungal counting consisted of glucose, 10 g/L; rose bengal, 0.033 g/L; KH_2PO_4, 1.0 g/L; $MgSO_4$ $7H_20$, 0.5 g/L; peptone, 5.0 g/L; agar, 20 g/L; and streptomycin, 30 mg/L (added through millipore filter after autoclave) dissolved in deionized water. The pH of the medium was adjusted to 6.8.

Results

Flow Cell A

Measured water flux through flow cell A decreased gradually from 1.6×10^{-5} m/s at the beginning of the experiment to 6.9×10^{-6} m/s at the end of the experiment (Figure 2), indicating a reduction of the average permeability of the system. Hydraulic head profiles along the flow cell (Figure 3) show that steepest gradients can be found in the vicinity of the inlet. However, it must be assumed that clogging of the inlet screen, an observation often made for clogging experiments (Baveye et al. 1998), contributes to the measured changes in head gradients. Furthermore, the head gradients observed in the vicinity of the outlet of the flow cell show an unstable pattern and might be affected by processes at the outlet screen or outside the flow cell too. Therefore, further analysis is focused on the inner part of the flow cell comprised between 4 and 16 cm from the inlet.

Comparing the average head gradients for the zone upstream from the nutrient injection port (4 to 10 cm from the inlet) with gradients observed for the zone downstream of the nutrient injection port (10 to 16 cm from the inlet) shows that toward the end of the experiment, larger gradients can be found in the downstream zone. Assuming a one-dimensional flow field allows the computation of hydraulic conductivities for both zones (Figure 4), showing that the hydraulic conductivity of the upstream zone remains nearly constant throughout the experiment. In contrast, the hydraulic conductivity of the downstream zone decreases within the first 4 d of the experiment to ~50% of its initial value, remaining on this reduced level until the end of the experiment. A comparison of observations for the subzones from 10 to 13 cm and from 13 to 16 cm showed similar results for each subzone (data not shown).

Biomass abundance was determined by measuring numbers of bacteria and fungi at the end of the experiment. Samples were taken at 4 and 10 cm distance from the inlet and were assumed to be representative for the

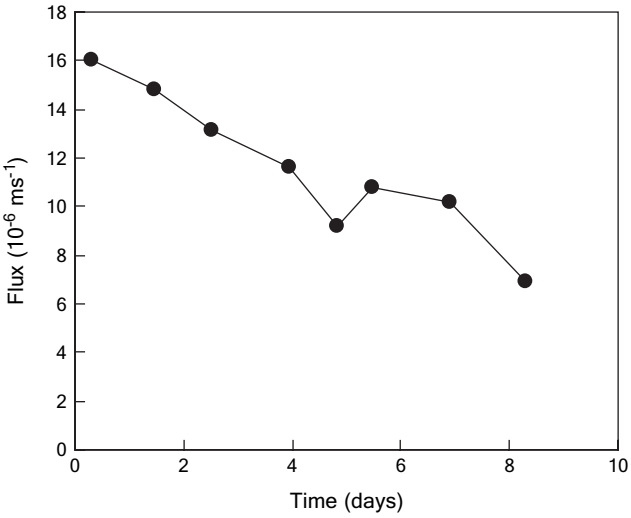

Figure 2. Flow cell A: flux changes during the experiment.

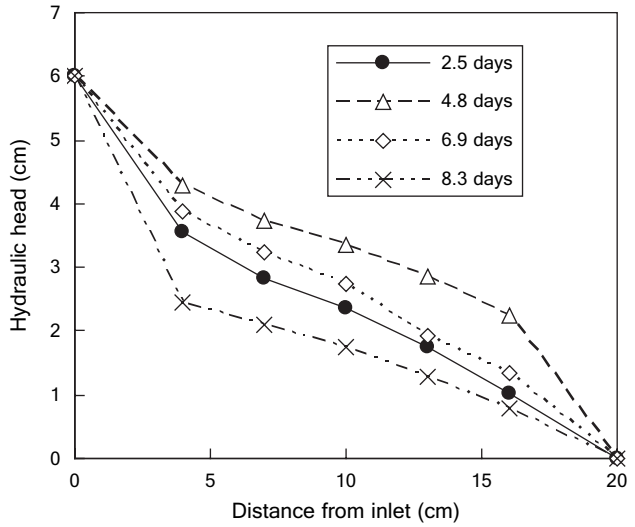

Figure 3. Flow cell A: hydraulic head profiles along the flow cell.

upstream and downstream zone, respectively. Numbers for both zones of flow cell A are shown in Table 1 together with the hydraulic conductivities of these zones at the beginning and the end of the experiment. In the downstream zone, where a decrease in hydraulic conductivity could be observed, numbers were ~2 (bacteria) and 3 (fungi) orders of magnitude higher than in the upstream zone, where the hydraulic conductivity remained unchanged.

Flow Cell B

Measured water flux through flow cell B decreased gradually from 2.2×10^{-5} m/s at the beginning of the experiment to 1.1×10^{-5} m/s at the end of the experiment (Figure 5), indicating that the average permeability of the flow cell decreased during the experiment. Hydraulic head

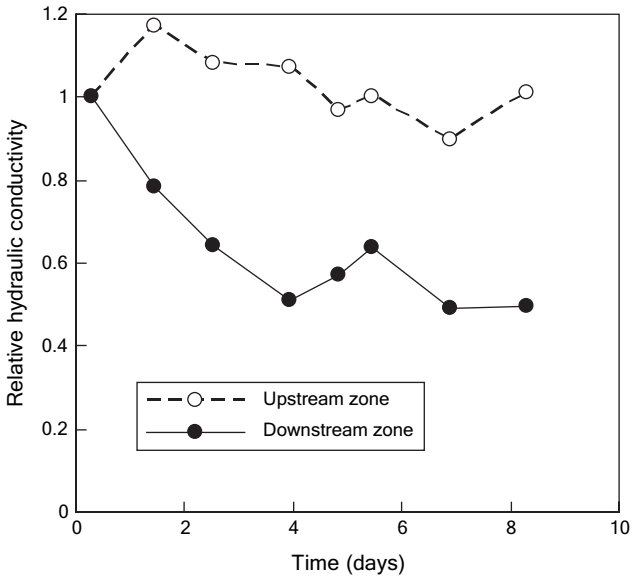

Figure 4. Flow cell A: relative hydraulic conductivity (K_s/K_{s0}) of the upstream zone (4 to 10 cm from inlet) and the downstream zone (10 to 16 cm from inlet).

Table 1
Flow Cell A: Initial and Final Hydraulic Conductivities Together with Numbers of Bacteria and Fungi

	Upstream Zone (4–10 cm)	Downstream Zone (10–16 cm)
Initial hydraulic conductivity (m/s)	6.00×10^{-5}	8.76×10^{-5}
Final hydraulic conductivity (m/s)	6.03×10^{-5}	4.34×10^{-5}
Numbers of bacteria (cells/g beads)	1.70×10^{5}	1.37×10^{7}
Numbers of fungi (cells/g beads)	6.30×10^{3}	4.26×10^{6}

profiles along the flow cell were calculated by averaging three manometer readings at each distance from the inlet (Figure 6). At the beginning of the experiment, the hydraulic gradient was approximately constant along the flow cell, whereas toward the end of the experiment, the hydraulic gradient was steeper in the vicinity of the inlet than in the inner parts of the column.

Hydraulic conductivities at the upstream zone (4 to 10 cm from the inlet) and the downstream zone (10 to 16 cm from the inlet) of the nutrient injection ports were calculated by the same method as flow cell A (Figure 7). Hydraulic conductivities slightly decreased in the upstream and downstream zone with the higher decrease observed for the downstream zone. For both zones, this decrease was not monotonous but fluctuated throughout the experiment.

The flow field in the flow cell B was further analyzed by tracer tests performed at 1.9, 2.9, 6.8, and 8.8 d after the beginning of the experiment (Figure 8). For the first three tracer tests, tracer solution was injected simultaneously into the three tracer injection ports, at 4 cm distance from inlet. For the last tracer test, at 8.8 d, the tracer

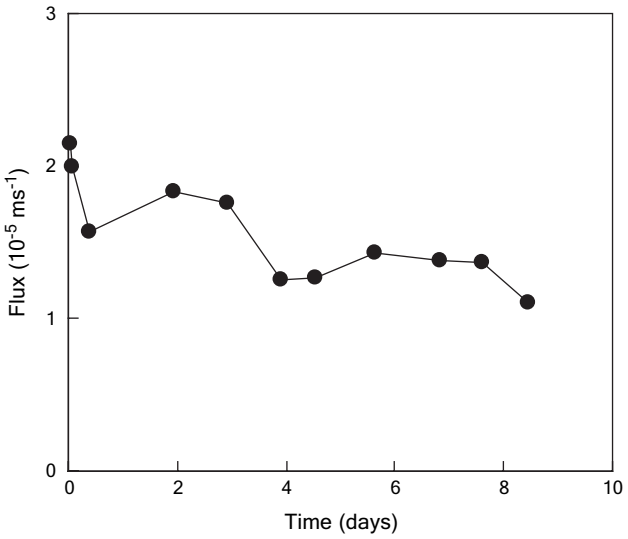

Figure 5. Flow cell B: flux changes during the experiment.

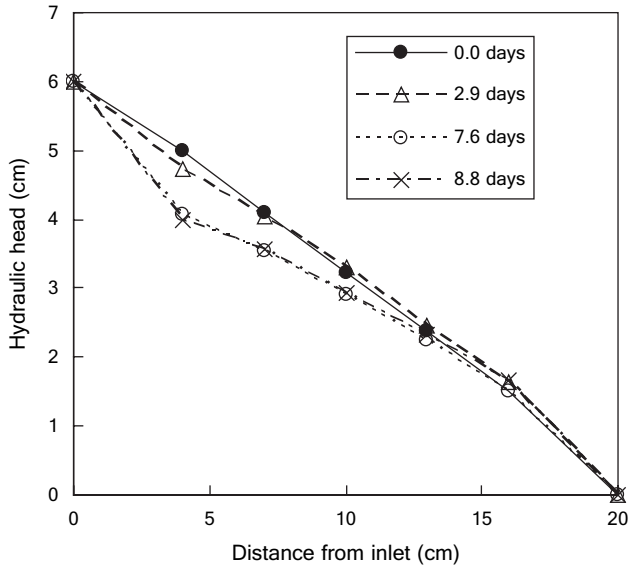

Figure 6. Flow cell B: hydraulic head profile along the flow cell as averaged by three manometer readings.

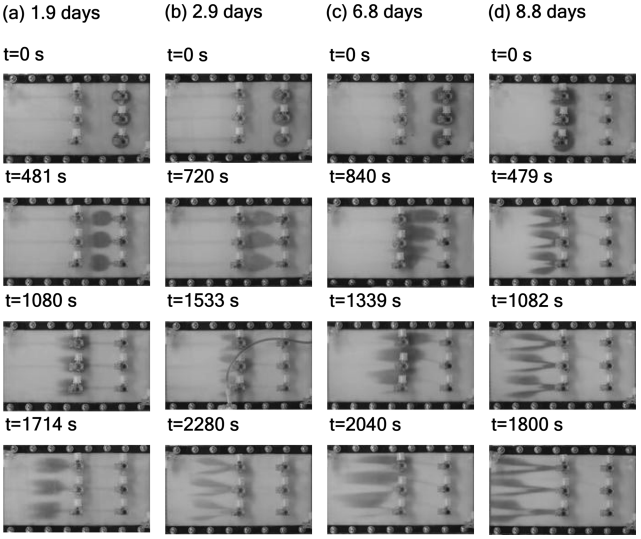

Figure 8. Flow cell B: tracer movement after 1.9, 2.9, 6.8, and 8.8 d. Light blue lines originating from the nutrient injection ports on some of the images are remainders from further tests.

solution was injected into the three nutrient injection ports, at 10 cm distance from inlet, to further visualize the flow paths in the vicinity of these ports. At 1.9 d (Figure 8a), a uniform flow field was observed in the entire column, with the nutrient injection ports themselves as the only disturbance for the tracer flow. At 2.9 d (Figure 8b), the tracer flow showed an increased flow barrier around each nutrient injection port causing the tracer to bypass the vicinity of the nutrient injection ports by splitting each tracer plume into two branches. At 6.8 d, the observation of a flow bypass of the nutrient injection ports was even more obvious (Figure 8c), and in addition, the total flow was diverted toward the upper direction of the shown images, i.e., the part of the flow cell to the right of the flow direction. At 8.8 d (Figure 8d), when the tracer was injected into the nutrient injection ports, flow bypass of an area directly downstream of the nutrient injection ports could be observed indicating a reduced conductivity in these zones. Nevertheless, in all tracer tests some of the injected tracer was entering the bypassed zones too.

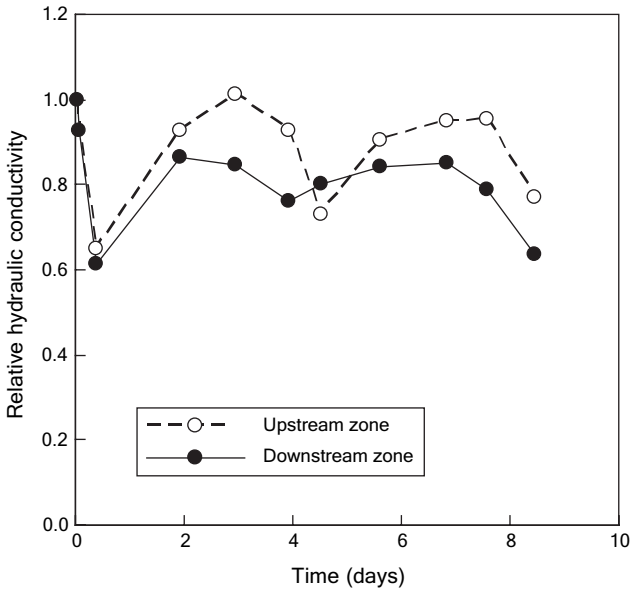

Figure 7. Flow cell B: relative hydraulic conductivity (K_s/K_{s0}) of the upstream zone (4 to 10 cm from inlet) and the downstream zone (10 to 16 cm from inlet).

To quantify the velocity of tracer movement in different parts of the flow cell, the position of the leading edge of parts of the tracer plumes was monitored at 8.8 d (Figure 9). Different parts of the tracer plumes were assumed to represent the tracer movement within the bypassed (bio)barrier (points 1, 2, and 3), in the flow paths bypassing the barrier (points 4 and 5) and the background flow (points 6 and 7; measured for a separate tracer test at the same day and same flow conditions, results not shown). Averaged values from the measurement points were fitted by linear regression to calculate velocities (Figure 9). Measured results indicate that velocity differences between the flow bypasses and the biobarrier were largest in a zone directly downstream of the nutrient injection ports (10 to 13 cm from the inlet). In this zone, the velocities in the bypasses are ~1 order of magnitude larger than velocities in the biobarrier and 2 to 3 times larger than the background velocity. Assuming that the zone downstream of the injection ports can be subdivided into two regions, a clogged biobarrier region and a region of unclogged preferential flow bypass, the following relations can be assumed for fluxes Q and cross sections A of these regions: $Q_p + Q_b = Q_0$ and $A_p + A_b = A_0$, with 0, p, and b indicating the background, preferential flow bypass, and biobarrier regions, respectively. Furthermore, assuming $Q = Avn$ for each region leads to $A_p v_p n_p + A_b v_b n_b = A_0 v_0 n_0$, with n as porosity and v as pore water or transport velocity. Substituting $A_b = A_0 - A_p$ in this equation and assuming that $n_p = n_0$ allows calculating the contribution of the preferential flow region

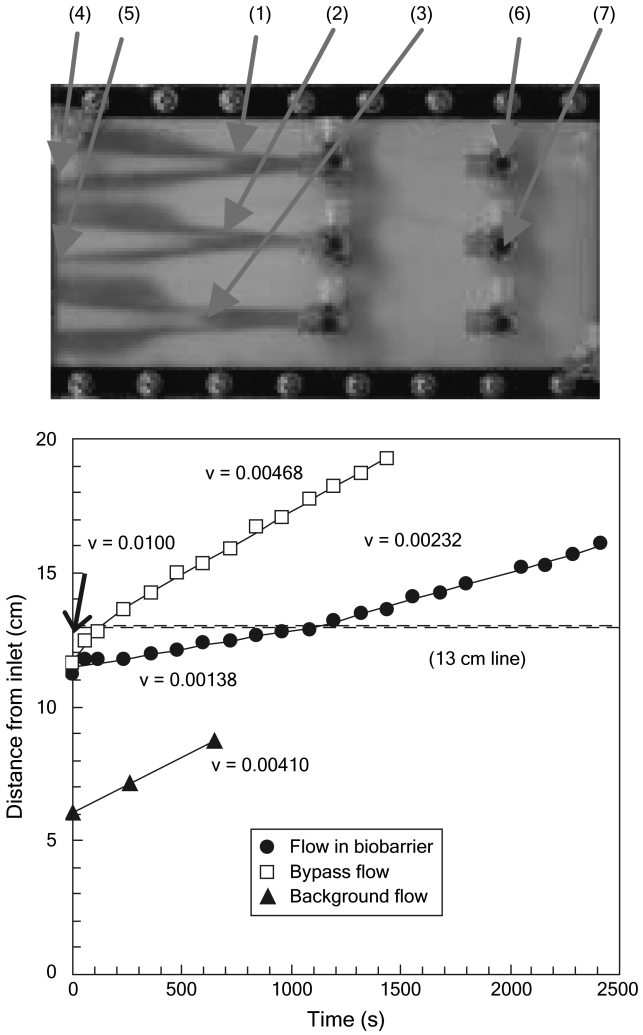

Figure 9. Flow cell B: tracer movement measured at different points after 8.8 d. Top: tracer distribution and parts of the tracer plume used for determination of velocities. Bottom: measured velocities of tracer migration. "Flow in biobarrier" is the average of points 1, 2, and 3; "Bypass flow" is the average of points 4 and 5; and "Background flow" is the average of points 6 and 7 in the top photo. Slopes of the linear regression are shown as v (in cm/s). For the biobarrier and the bypass flow, linear regressions were determined independently for points before and behind a line 13 cm from the column inlet.

to the total water flux given as:

$$\frac{Q_p}{Q_0} = \frac{v_p A_p}{v_0 A_0} = \frac{v_p}{v_0} \frac{(v_0 n_0 - v_b n_b)}{(v_p n_0 - v_b n_b)}$$

Using velocity values measured for the zone 10 to 13 cm from the inlet and for the background, and neglecting porosity changes in the biobarrier results in ~77% of the water flowing through this zone via preferential flow bypass. Considering a porosity reduction in the biobarrier to 80% of its initial value (a realistic assumption for the moderate clogging level observed in this study; Vandevivere et al. 1995; Thullner et al. 2002b) results in the flow bypass contributing 82% to the total water flux.

Further downstream, the velocity of the bypass decreased to values close to the background velocity, whereas the velocities in the biobarrier increased but still remained a factor of 2 smaller than the bypass velocity.

After the flow was terminated, bacteria and fungi were counted for two samples taken directly downstream of a nutrient injection port, and one sample taken from the middle of a zone between two nutrient injection ports. Samples taken downstream of the injection ports show that cell numbers for bacteria and fungi were 2 orders of magnitudes higher than cell numbers obtained for the sample taken between the injection ports (Table 2).

Discussion

Hydraulic Conductivity Changes Caused by Microorganisms

Changes in the hydraulic properties of the porous medium could be observed in both flow cells throughout the experiments. In particular, these changes resulted in a reduction of the average hydraulic conductivity of the media and, in the case of flow cell B, in a modification of the flow pattern in the cell. The occurrence of these hydraulic effects was spatially correlated with the position of the nutrient injection ports and was attributed to the observed increase in the abundance of microorganisms by 2 to 3 orders of magnitude in the vicinity of these ports. Mineral precipitation was unlikely to occur as a complete mineralization of the injected glucose would not result in a CO_3^{2-} concentration of more than 0.016 mM (assuming the pH not raising above 7). Even for $MgCO_3$, the least soluble of the potential precipitates in the flow cell, the ionic product would not exceed 1.3×10^{-8}, which is ~2 orders of magnitude below the solubility product of this mineral or its hydrates (2.4×10^{-6} to 6.8×10^{-6}; Lide 1999). All other potentially forming carbonates (K_2CO_3, $KHCO_3$, Na_2CO_3, and $NaHCO_3$) are highly soluble and, thus, not precipitating at the given conditions too. Generally, no indications were observed for mineral precipitation or particle deposition as an alternative reason for the observed effects, supporting the assumption of bioclogging being the only cause of the changes in hydraulic properties of the porous media. Furthermore, the bioclogging effect is attributed to the buildup of microbial biomass (i.e., microbial cells, extracellular polymeric substances [EPS]) and not to the formation of biogenic gas bubbles as no indications were found for any gas formation in the flow cells.

Table 2
Flow Cell B: Numbers of Bacteria and Fungi

	Outside Streamline	Inside Streamline[1]
Numbers of bacteria (cells/g beads)	3.93×10^5	3.34×10^7
Numbers of fungi (cells/g beads)	1.83×10^4	1.85×10^6

[1]Average of two nutrient ports.

The bioclogging observed in flow cell A resulted in a decrease in hydraulic conductivity of ~50%, which is relatively moderate compared to hydraulic conductivity changes of 2 to 3 orders of magnitude observed in other bioclogging experiments with a one-dimensional flow field (e.g., Taylor and Jaffé 1990; Cunningham et al. 1991; Vandevivere and Baveye 1992a; Seki et al. 1998). As it has been shown in previous studies that in bioclogged systems the clogging is mainly caused by EPS or other by-products of microbial growth (Vandevivere and Baveye 1992b; Thullner et al. 2002a), the measured numbers of microorganisms do not allow the evaluation of whether this moderate clogging was due to smaller amounts of biomass or a smaller clogging efficiency of the produced biomass compared to other clogging experiments. For the two-dimensional flow field in flow cell B, the measured average changes in the hydraulic conductivity do not provide a reliable estimate of local changes of this parameter. However, the fact that the injected tracer ultimately entered the clogged areas, too, suggests that also for flow cell B the clogging locally reached only moderate levels. Similar observations have been made previously by Kildsgaard and Engesgaard (2002) and Thullner et al. (2002a) in clogging experiments using two-dimensional flow fields. However, it should be noted that in a subsequent modeling study Thullner et al. (2004) could reproduce the results of Thullner et al. (2002a) while showing that high reductions in hydraulic conductivity by ~2 orders of magnitude in a narrow clogging zone allowed a tracer dye entering the area enveloped by the bioclogged zone.

Comparison of One- and Two-Dimensional Flow Fields

Besides the widths of the flow cell, the experimental setup for flow cell A and flow cell B was basically identical not providing further cause for differences between the clogging effects than those attributed to the different flow fields. In flow cell A, the flow field is assumed to be one dimensional. This assumption is challenged by the nutrient injection port being a point source in a homogenous background flow field, but the small width of the flow cell (1 cm) is taken as justification for the applied simplification. Using this assumption and taking into account that in the downstream zone the average hydraulic conductivity reduction did not change significantly along the flowpath indicate that the average hydraulic conductivity change provides a reasonable estimate for bioclogging effects occurring locally. This suggests that the changes of hydraulic conductivity were moderate on the local scale too.

Extrapolating the results from flow cell A to flow cell B it can be assumed that locally the impact of the microorganisms on the hydraulic conductivity was approximately the same. This assumption is supported by the numbers of microorganisms measured for the clogged downstream zone of flow cell A and inside the clogged nutrient port streamlines for flow cell B. For bacteria and fungi, these numbers differ only by a factor of 2 between the different flow cells, whereas numbers for the unclogged areas were 2 orders of magnitude smaller. However, in contrast to flow cell A, the average hydraulic conductivity measured for the zones upstream and downstream of the nutrient injection ports in flow cell B were quite similar hardly indicating any clogging effects to occur. The flow field observed during the tracer tests performed for flow cell B demonstrates that the clogging was changing the flow from an initially quite homogeneous pattern toward a preferential flow pattern with a succession of clogged areas and flow paths bypassing the clogged areas along the width of the flow cell. The number of microorganisms and flow velocities determined for different flow paths during a tracer test indicate that the contrast in hydraulic conductivity between clogged and unclogged areas along the width of flow cell B is similar to the contrast observed between the clogged and unclogged zones in flow cell A. This demonstrates that despite the small scale of the experimental setup, a homogeneous flushing of the flow cell was prevented by the bioclogging. The observation of steep spatial gradients in biomass concentration was also reported by Thullner et al. (2002a), but using a different nutrient supply system. In contrast to other small-scale experiments (e.g., Stewart and Fogler 2002), the sharp contrast we observed between clogged and unclogged areas on a mm to cm scale was not caused by a constant flux setup, where increasing shear forces results in preferential flow paths through a clogged porous media. In addition, the clogged areas are assumed to be clogged only moderately. These results indicate that even in small-scale setups, moderate levels of bioclogging can lead to a preferential flow pattern, with bioclogged areas bypassed by preferential flow paths. As a consequence, measuring the average hydraulic conductivity on a larger scale does not allow detecting the occurrence of bioclogging in such a case. Finally, these findings indicate that results obtained from column experiments assumed to have a one-dimensional flow field provide only limited information on the occurrence of bioclogging effects in two-dimensional flow fields.

Implications for Clogging Effects in Field-Scale Biobarriers

Transferring the results from laboratory experiments to the field and to the application of biobarriers is challenged by the differences in the spatial and temporal scales and in experimental conditions such as the hydraulic gradient. In the field, hydraulic gradients would be much smaller than in the present experiment, resulting in smaller rates of nutrient supply and biomass growth. Therefore, the period required for biomass accumulation being sufficiently high for bioclogging would be longer than observed in the present laboratory experiments. This and the difference in the spatial scale suggest that in the field, bioclogging effects occur on a larger time scale than observed in the flow cells. However, there were no indications that the effects presented here—bioclogging-induced preferential flow patterns within a PRB—would not generally take place under field conditions too. Actually, most bioclogging studies so far were performed in the laboratory and hardly any quantitative data are available on the occurrence of bioclogging on the field scale. As a consequence, up to now the prediction of bioclogging and its implications on the performance of biobarriers is based on data from the laboratory. The performance of biobarriers is tested by model predictions and the breakthrough of reactive and nonreactive

tracers measured at selected observation points downstream of the barrier (e.g., Hyndman et al. 2000; Dybas et al. 2002). These approaches are certainly limited by the occurrence of flow field heterogeneities caused by the aquifer material at a site (Bilbrey and Shafer 2001). Our experiments show that even in the absence of these initial heterogeneities, the occurrence of bioclogging can lead to a heterogeneous flow pattern. The increased travel velocities in these paths would reduce the residence time of any contaminants in a biobarrier, thus limiting the barrier's ability to degrade the contaminants. Our results indicate that even moderate bioclogging can cause such an effect, i.e., in our case at least 77% of the flow passed the barrier via the preferential paths. Furthermore, the observed spreading of the injected tracer showed that detecting such a preferential flow pattern might highly depend on the position of observation points and that a high number of these points might be needed to resolve the flow pattern downstream of a biobarrier and consequently the evaluation of a biobarrier's performance might require a higher number of observation points than commonly used. In addition, our observations emphasize the importance of using an appropriate nutrient delivery system within a biobarrier. This delivery system must support a smooth distribution of microorganisms within the biobarrier avoiding hot spots of microbial activity as they can lead to the observed bioclogging effects.

Conclusions

This study addressed the impact hydraulic conductivity changes due to bioclogging can have on the flow pattern in an engineered biobarrier. Results obtained from laboratory-scale flow cell experiments having a two-dimensional flow field indicate that even for nutrient supplies leading to moderate clogging, only, the flow field in the biobarrier exhibits preferential flow paths. These flow paths are the main contributors to water flow through the biobarrier, and the increased velocities in these paths lead to a decreased residence time of water and its constituents in these biobarriers. The average hydraulic conductivity of the entire barrier was hardly affected by the bioclogging suggesting that a detection of such clogging effects in the field might require a high spatial resolution of the monitoring system even at sites with no initial heterogeneities to allow detecting the occurrence of preferential flow paths developing during the operation of the biobarrier. Furthermore, these results suggest that the performance of PRB used for the bioremediation of contaminated ground water does require a homogeneous growth of organisms not only to increase the contact between microorganisms and contaminants but also to avoid the occurrence of hot spots of microbial growth, which would lead to a preferential flow pattern within the biobarrier. Observations from this study show that information from column experiments on bioclogging assuming a one-dimensional flow field is already of limited use for predicting bioclogging effects in two-dimensional flow fields. Predicting the impact bioclogging might have on PRBs should not be done based on such column experiments, and more research is recommended to investigate these clogging effects in the field directly.

Acknowledgment

Technical assistance by Hiromi Imoto at the University of Tokyo is appreciated.

References

Baveye, P., P. Vandevivere, B.L. Hoyle, P.C. DeLeo, and D. Sanchez de Lozada. 1998. Environmental impact and mechanisms of the biological clogging of saturated soils and aquifer materials. *Critical Review in Environmental Science and Technology* 28, no. 2: 123–191.

Bilbrey, L.C., and J.M. Shafer. Funnel-and-gate performance in a moderately heterogeneous flow domain. 2001. *Ground Water Monitoring and Remediation* 21, no. 3: 144–151.

Cunningham, A.B., W.G. Characklis, F. Abedeen, and D. Crawford. 1991. Influence of biofilm accumulation on porous media hydrodynamics. *Environmental Science and Technology* 25, no. 7: 1305–1311.

Davis, S., W. Fairbank, and H. Weisheit. 1973. Dairy waste ponds effectively self-sealing. *Transactions of the ASAE* 16, no. 1: 69–71.

Dybas, M.J., D.W. Hyndman, R. Heine, J. Tiedje, K. Linning, D. Wiggert, T. Voice, X. Zhao, L. Dybas, and C.S. Criddle. 2002. Development, operation, and long-term performance of a full-scale biocurtain utilizing bioaugmentation. *Environmental Science and Technology* 36, no. 16: 3635–3644.

Gavaskar, A.R. 1998. *Permeable Barriers for Groundwater Remediation; Design Construction and Monitoring*. Columbus, Ohio: Battelle Press.

Hiebert, R., R. Sharp, A. Cunningham, and G. James. 2001. Development and demonstration of subsurface biofilm barriers using starved bacterial cultures. *Soil, Sediment & Water.*

Hyndman, D.W., M.J. Dybas, L. Forney, R. Heine, T. Mayotte, M.S. Phanikumar, G. Tatara, J. Tiedje, T. Voice, R. Wallace, D. Wiggert, X. Zhao, and C.S. Criddle. 2000. Hydraulic characterization and design of a full scale biocurtain. *Ground Water* 38, no. 3: 462–474.

Kalin, R.M. 2004. Engineered passive bioreactive barriers: Risk-managing the legacy of industrial soil and groundwater pollution. *Current Opinion in Microbiology* 7, no. 3: 227–238.

Kildsgaard, J., and P. Engesgaard. 2002. Tracer test and image analysis of biological clogging in a two-dimensional sandbox experiment. *Ground Water Monitoring and Remediation* 22, no. 2: 60–67.

Kristiansen, R. 1981. Sand-filter trenches for purification of septic tank effluent: The clogging mechanism and the soil physical environment. *Journal of Environmental Quality* 10, no. 3: 353–357.

Lide, E.R, ed. 1999. *CRC Handbook of Chemistry and Physics*, 80th ed. New York: CRC Press.

McCarty, P.L., M.N. Goltz, G.D. Hopkins, M.E. Dolan, J.P. Allan, B.T. Kawakami, and T.J. Carrothers. 1998. Full-scale evaluation of in situ cometabolic degradation of trichloroethylene in groundwater through toluene injection. *Environmental Science and Technology* 32, no. 1: 88–100.

Oberdorfer, J.A., and F.L. Peterson. 1985. Wastewater injection—Geochemical and biogeochemical clogging processes. *Ground Water* 23, no. 6: 753–761.

Rebhun, M., and J. Schwarz. 1968. Clogging and contamination processes in recharge wells. *Water Resources Research* 4, no. 6: 1207–1217.

Scherer, M.M., S. Richter, R.L. Valentine, and P.J.J. Alvarez. 2000. Chemistry and microbiology of permeable reactive barriers for in situ groundwater clean up. *Critical Reviews in Microbiology* 26, no. 4: 221–264.

Seki, K., T. Miyazaki, and M. Nakano. 1998. Effects of microorganisms on hydraulic conductivity decrease in infiltration. *European Journal of Soil Science* 49, no. 2: 231–236.

Stewart T.L., and H.S. Fogler. 2002. Pore-scale investigation of biomass plug development and propagation in porous media. *Biotechnology and Bioengineering* 77, no. 5: 577–588.

Taylor, S.W., and P.R. Jaffé. 1990. Biofilm growth and the related changes in the physical properties of a porous medium. 1. Experimental Investigation. *Water Resources Research* 26, no. 9: 2153–2159.

Thullner, M., L. Mauclaire, M.H. Schroth, W. Kinzelbach, and J. Zeyer. 2002a. Interaction between water flow and spatial distribution of microbial growth in a two-dimensional flow field in saturated porous media. *Journal of Contaminant Hydrology* 58, no. 3–4: 169–189.

Thullner, M., M.H. Schroth, J. Zeyer, and W. Kinzelbach. 2004. Modeling of a microbial growth experiment with bioclogging in a two-dimensional saturated porous media flow field. *Journal of Contaminated Hydrology* 70, no. 1–2: 37–62.

Thullner M., J.. Zeyer, and W. Kinzelbach. 2002b. Influence of microbial growth on hydraulic properties of pore networks. *Transport in Porous Media* 49, no. 1: 99–122.

Trefry, M.G., J.L. Rayner, and C.D. Johnston. 1998. Hydrological measures of success for a pilot bioclogging study at Largs North, South Australia. CSIRO Land and Water, Technical Report 24/98. Collingwood, Victoria, Australia: CSIRO.

van Beek, C.G.E.M., and D. van der Kooij. 1982. Sulfate-reducing bacteria in ground water from clogging and non-clogging shallow wells in the Netherlands river region. *Ground Water* 20, no. 3: 298–302.

Vandevivere, P., and P. Baveye. 1992a. Saturated hydraulic conductivity reduction caused by aerobic bacteria in sand columns. *Soil Science Society of America Journal* 56, no. 1: 1–13.

Vandevivere, P., and P. Baveye. 1992b. Effect of bacterial extracellular polymers on the saturated hydraulic conductivity of sand columns. *Applied and Environmental Microbiology* 58, no. 5: 1690–1698.

Vandevivere, P., P. Baveye, D. Sanchez de Lozada, and P. DeLeo. 1995. Microbial clogging of saturated soils and aquifer materials: Evaluation of mathematical models. *Water Resources Research* 31, no. 9: 2173–2180.

Vecchioli, J. 1970. A note on bacterial growth around a recharge well at Bay Park, Long Island, New York. *Water Resources Research* 6, no. 5: 1415–1419.

Weaver, R.W., S. Angle, P. Bottomley, D. Bezdicek, S. Smith, A. Tabatabai, and A. Wollum. 1994. *Methods of Soil Analysis. Part 2. Microbiological and Biochemical Properties*. Madison, Wisconsin: Soil Science Society of America.

Biographical Sketches

Katsutoshi Seki, *Ph.D., corresponding author, is an assistant professor at the Laboratory of Soil Physics and Soil Hydrology, Department of Biological and Environmental Engineering, Graduate School of Agricultural and Life Sciences, the University of Tokyo, Yayoi 1-1-1, Bunkyo-ku, Tokyo 113-8657, Japan; (81) 3-5841-5352; fax (81) 3-5841-8171; seki@soil.en.a.u-tokto.ac.jp. His research interests include water transport in saturated and unsaturated porous media.*

Martin Thullner, *Ph.D., is a research scientist at the Department of Environmental Microbiology, UFZ Centre for Environmental Research Leipzig-Halle, Permoserstr. 15, 04138 Leipzig, Germany; martin.thullner@ufz.de. His research interests include reactive transport in porous media and numerical modeling.*

Junya Hanada, *M.S., is a government employee at the Ministry of Agriculture, Forestry and Fisheries of Japan, Jasumigaseki 1-2-1, Chiyoda-ku, Tokyo 100-8950, Japan.*

Tsuyoshi Miyazaki, *Ph.D., is a professor at the Laboratory of Soil Physics and Soil Hydrology, Department of Biological and Environmental Engineering, Graduate School of Agricultural and Life Sciences, the University of Tokyo, Yayoi 1-1-1, Bunkyo-ku, Tokyo 113-8657, Japan; amiyat@soil.en.a.u-tokyo.ac.jp. He is the author of* Water Flow in Soils, *second edition, published by CRC Press in 2006.*